

Published in final edited form as:

Invest Ophthalmol Vis Sci. 2008 January ; 49(1): 320–332. doi:10.1167/iovs.07-0593.

Modeling of Corneal and Retinal Pharmacokinetics after Periocular Drug Administration

Aniruddha C. Amrite^{1,2}, Henry F. Edelhauser³, and Uday B. Kompella^{1,4}

¹Department of Pharmaceutical Sciences, University of Nebraska Medical Center, Omaha, Nebraska

³Emory Eye Center, Emory University, Atlanta, Georgia.

⁴Department of Ophthalmology and Visual Sciences, University of Nebraska Medical Center, Omaha, Nebraska

Abstract

Purpose—To develop pharmacokinetics models to describe the disposition of small lipophilic molecules in the cornea and retina after periocular (subconjunctival or posterior subconjunctival) administration.

Methods—Compartmental pharmacokinetics analysis was performed on the corneal and retinal data obtained after periocular administration of 3 mg of celecoxib (a selective COX-2 inhibitor) to Brown Norway (BN) rats. Berkeley Madonna, a differential and difference equation-based modeling software, was used for the pharmacokinetics modeling. The data were fit to different compartment models with first-order input and disposition, and the best fit was selected on the basis of coefficient of regression and Akaike information criteria (AIC). The models were validated by using the celecoxib data from a prior study in Sprague-Dawley (SD) rats. The corneal model was also fit to the corneal data for prednisolone at a dose of 2.61 mg in albino rabbits, and the model was validated at two other doses of prednisolone (0.261 and 26.1 mg) in these rabbits. Model simulations were performed with the finalized model to understand the effect of formulation on corneal and retinal pharmacokinetics after periocular administration.

Results—Celecoxib kinetics in the BN rat cornea can be described by a two-compartment (periocular space and cornea, with a dissolution step for periocular formulation) model, with parallel elimination from the cornea and the periocular space. The inclusion of a distribution compartment or a dissolution step for celecoxib suspension did not lead to an overall improvement in the corneal data fit compared with the two-compartment model. The more important parameter for enhanced fit and explaining the apparent lack of an increase phase in the corneal levels is the inclusion of the initial leak-back of the dose from the periocular space into the precorneal area. The predicted celecoxib concentrations from this model also showed very good correlation ($r = 0.99$) with the observed values in the SD rat corneas. Similar pharmacokinetics models explain drug delivery to the cornea in rat and rabbit animal models. Retinal pharmacokinetics after periocular drug administration can be explained with a four-compartment (periocular space, choroid-containing transfer compartment, retina, and distribution compartment) model with elimination from the periocular space, retina, and choroid compartment. Inclusion of a dissolution-release step before the drug is available for absorption or elimination better explains

Copyright © Association for Research in Vision and Ophthalmology

Corresponding author: Uday B. Kompella, University of Nebraska Medical Center, Omaha, NE 68198-5840; ukompell@unmc.edu..

²Present affiliation: Quintiles Inc., Overland Park, Kansas.

Disclosure: A.C. Amrite, None; H.F. Edelhauser, None; U.B. Kompella, Pfizer (F)

retinal t_{\max} . Good fits were obtained in both the BN ($r = 0.99$) and SD ($r = 0.99$) rats for retinal celecoxib using the same model; however, the parameter estimates differed.

Conclusions—Corneal and retinal pharmacokinetics of small lipophilic molecules after periocular administration can be described by compartment models. The modeling analysis shows that (1) leak-back from the site of administration most likely contributes to the apparent lack of an increase phase in corneal concentrations; (2) elimination via the conjunctival or periocular blood and lymphatic systems contributes significantly to drug clearance after periocular injection; (3) corneal pharmacokinetics of small lipophilic molecules can be explained by using similar models in rats and rabbits; and (4) although there are differences in some retinal pharmacokinetics parameters between the pigmented and nonpigmented rats, the physiological basis of these differences has yet to be ascertained.

Drug delivery by the topical route, although effective for anterior segment disorders, does not result in significant retinal concentrations of most molecules.¹ Because it is a safer approach, the periocular route of drug delivery is gaining importance as an alternative to the intravitreal route for the treatment of posterior segment ocular disorders. The periocular routes include the subconjunctival, subtenon, peribulbar, and retrobulbar modes.² Although these routes deliver drugs to the posterior segment tissues including the retina and the vitreous, the bioavailability of the route is not clearly established. Literature on the pharmacokinetics of periocular injections is relatively sparse compared with that on the topical or intravitreal modes of administration. Understanding the pharmacokinetics is essential for determining the dose regimen and for designing novel drugs and delivery systems.

Pharmacokinetic modeling is a powerful tool for a better understanding of drug disposition. There have been some attempts to perform mathematical modeling of periocular injections. These approaches for posterior segment delivery have been summarized by Pekka-Ranta and Urtii.³ Tsuji et al.⁴ described the pharmacokinetics of a small lipophilic steroid (prednisolone) in tissues of the anterior and posterior segments. However, the model development procedure was not described, and there were no statistical goodness-of-fit criteria mentioned, and thus the use of their model is limited. Lee and Robinson⁵ developed a model that describes the pharmacokinetics in the vitreous after periocular administration.⁵ The model was developed with the data of Tsuji et al.⁴ Most of the posterior segment disorders affect the retina and/or the choroid, and no model has been developed to date to describe the pharmacokinetics of the drugs in the retina. There is significant drug delivery to the anterior segment after subconjunctival administration.^{6–8} However, attempts to model the pharmacokinetics of drugs in the cornea after subconjunctival or other periocular modes of administration have been few.

Modeling software is an important consideration in developing any mathematical model. Berkeley Madonna (Berkeley Madonna, Berkeley, CA) is a commercially available modeling software that numerically solves ordinary differential equations. It has a user friendly graphic user interface (GUI) and the users can modify the model by diagrammatic modification. Differential equations are directly developed and solved by the software (www.berkeleymadonna.com/BM%20User's%20Guide%208.0.pdf). The software has powerful algorithms for achieving convergence and has been used extensively in the development of multicompartment, multiparametric models such as physiologically based pharmacokinetics models (PBPK).^{9,10} The modeling software allows for both the forward-modeling approach (simulation) and backward-modeling approaches (parameter estimations using curve fitting). Thus, the purpose of this study was to use Berkeley Madonna and the compartment approach to pharmacokinetic modeling, to explain the pharmacokinetics of small lipophilic molecules in the cornea and retina after periocular administration.

Materials and methods

Modeling Software

The mathematical compartment modeling of the pharmacokinetic data was performed with the Berkeley Madonna software. The model parameters were estimated by using the curve-fitting procedure in the software. The integration step size was fixed at 0.02 minutes and the Runge-Kutta 4 method was used as the integration method in all the models tested.

Datasets for Modeling and Model Validation

Modeling was performed for two different tissues: cornea (anterior segment) and retina (posterior segment). Data for pharmacokinetic modeling were obtained from three studies. Initial model fitting was performed for the cornea and retina celecoxib data reported by Cheruvu et al.¹¹ in pigmented Brown Norway (BN) rats after posterior subconjunctival injection. The corneal model was validated by using the pharmacokinetic data that Ayalasmayajula and Kompella¹² obtained in nonpigmented Sprague-Dawley (SD) rats after a similar injection, and further comparisons and validations were performed with the prednisolone corneal pharmacokinetics data of Tsuji et al.⁴ after subconjunctival injection in albino rabbits. The retinal model developed with the BN rat data¹¹ was validated with the SD rat data of Ayalasmayajula and Kompella.¹²

Model Development

The model was developed in an approach similar to the forward stepwise modeling used in linear regression. We started with the simplest model to describe the pharmacokinetics and added additional components (compartments/parameters/equations) to improve the fits to the data. The model was finally selected on the basis of a better statistical fit compared with the simpler model.

Model Application to Simulate the Influence of Various Formulations on Corneal and Retinal Drug Levels

We applied the models developed for a 3-mg celecoxib suspension to hypothetical solution and sustained-release dosage forms. The doses for the solution and sustained-release formulations were fixed at 3 mg, and the drug release rates were varied relative to the fitted values obtained with the 3-mg celecoxib suspension. For the solution dosage form, the release rate was assumed to be infinite and instantaneous. For the sustained-release formulation, the release rate was assumed to be 1000-fold lower than that of the celecoxib suspension formulation. For the purpose of this simulation, clearance of the sustained-release system was assumed to be negligible.

Statistics

The model was selected on the basis of goodness-of-fit criteria such as the coefficient of determination (similar to a regression coefficient) and Akaike information criteria (AIC). A greater coefficient of determination and a lower AIC value indicate a better statistical fit. The formulas used for the calculation of these parameters are as follows:

$$\text{Coefficient of determination } (R^2) = 1 - [(n-1)/(n-p)] \left[\frac{(\sum Y_i - Y_i'')^2}{(\sum Y_i - Y_i')^2} \right] \quad (1)$$

and

$$\text{AIC} = n \cdot \log(\sum Y_i - Y_i')^2 + 2p, \quad (2)$$

where, n is the number of observations, Y_i is the observed value; Y_i' is the model-predicted value, Y_i'' is the mean of the observed values, and p is the number of model parameters.

In addition, the correlation coefficient was calculated with the finalized model whenever model validation was used. The correlation coefficient is not a goodness-of-fit metric. The formula for the correlation coefficient is

$$\text{Correlation coefficient } (r) = \frac{\sum (Y_i - Y_i'')(X_i - X_i'')}{\sqrt{\left[\sum (X_i - X_i'')^2 \cdot \sum (Y_i - Y_i'')^2 \right]} \quad (3)$$

where Y_i is the observed value, Y_i'' is the mean of the observed values, X_i is the predicted value, and X_i'' is the mean of the predicted values.

Results and Discussion

Model Selection for Corneal Pharmacokinetics after Periocular Drug Administration

In this study, we first developed a compartment model with data obtained in pigmented rats¹¹ and then validated the same with data from nonpigmented rats.¹² There is significant delivery of drugs to the cornea after subconjunctival administration.⁶ The cornea is devoid of circulation, and hence very little drug is expected to reach the cornea from the circulation. Our earlier studies showed that ~97% of drug delivery to the cornea after periocular administration is mainly by local pathways, as opposed to delivery via systemic circulation.¹² Hence, we started with a simple model whereby the drug had a local delivery pathway from the site of administration to the cornea after periocular administration (Fig. 1A). This base model consisted of two compartments, one representing the periocular site (which is made up of the periocular space and the tissue) and the other representing the cornea. It has been demonstrated in several studies that there is a significant loss of drug from periocular administration due to the presence of the conjunctival circulation and lymphatics.^{13–15} Hence, in our base model, we assumed an elimination pathway for the drug from the subconjunctival/periocular site. Also, it is possible that drugs are eliminated from the cornea possibly through tear turnover and blinking. Therefore, we assumed a corneal elimination pathway for the drugs. We assumed first-order kinetics wherein the rates of disposition are proportional to drug concentration. The model fit with this simple two-compartment model is shown in Figure 1A. The model fit to the experimental data was poor (R^2 : 0.41; AIC: 286.5) for the later time points and the estimates of the model parameters are therefore of little value. A visual examination of the elimination phase in the experimental corneal data of celecoxib clearly shows the existence of a distribution phase (bi- or multi-phasic kinetics). Studies have indicated the existence of a possible distribution compartment for pilocarpine in the anterior segment tissues.¹⁶ Theoretical discussions of modeling have described the existence of a distribution compartment comprising the aqueous.¹⁷ Therefore, we introduced a distribution compartment for the drug in the cornea. This distribution compartment is most likely a combination of aqueous humor and other anterior segment tissues such as the iris ciliary body. When the curve-fitting procedure was performed with this new model, the data-fits significantly improved at the later time points (Fig. 1B). The overall fit also improved significantly (R^2 : 0.5; AIC: 280.7). However, some initial data points could not be fit by either of the models described.

In the rat pharmacokinetics studies with celecoxib, the drug was administered as a suspension. A suspension formulation as opposed to a solution can have significant effects on the disposition of drugs in a particular tissue. Therefore, we included a dissolution or drug-release step in the celecoxib suspension formulation. The inclusion of this step actually did not lead to a significant improvement in the model fits. After including the drug

dissolution or release rate, the fit with the compartment model (R^2 : 0.29; AIC: 291.3) without a distribution compartment was better than that obtained with the inclusion of a distribution compartment (R^2 : 0.1; AIC: 327.4; Figs. 1C, 1D). We considered an additional model in which there are three elimination pathways, one from the periocular space, one from the cornea, and one from the distribution compartment (aqueous humor; Fig. 1G). However, the fit with this model was worse than the fit with any of the models described herein.

When the drug is administered by the periocular route, there can be significant leak-back into the cornea of the administered formulation along the needle tract.^{18–20} This leak-back is dependent on the method and location of subconjunctival injection and on the volume injected, with greater volumes leading to greater leak-back. In our experience, we have consistently observed that a fraction of the injected volume immediately accesses the cornea as the needle is withdrawn after posterior subconjunctival administration to rats. A similar leak-back has been reported in rabbits.^{18,19} Sasaki et al.^{18,19} have demonstrated that tilosolol as well as larger molecules (11 kDa FITC-dextran) leak out into the tear film after subconjunctival administration, which means that there is an initial bolus or higher delivery of dose to the cornea that should be incorporated in the model. To account for this initial drug load on the cornea, we used the models in Figure 1C, but allowed the initial concentration in the cornea to be an additional parameter to be estimated by the software. With this modification, the model was refit to the data (Fig. 1E; R^2 : 0.91; AIC: 225.2). There was a significant improvement in the model fits with this approach. The data fit the model well and the correlation coefficient between the observed and predicted values was excellent ($r = 0.99$).

When an additional source of drug was added to the base compartment model (model in Fig. 1C) and other models described herein, a significant improvement in the fits was observed (compare Figs. 1C, 1D, 1G with 1E, 1F, 1H, respectively). However, based on the lower AIC values, the same coefficient of determination, and a lower number of parameters, the model in Figure 1E is the best model among the ones assessed. This model was selected as the final one for explaining rat corneal disposition of celecoxib after periocular injection.

Recent studies by Kim et al.²¹ and Lee et al.²² have demonstrated that episcleral implants of cyclosporine can deliver high levels of the drug to the rabbit cornea. The implants also show beneficial therapeutic effects in the lachrymal glands of other species including the canine model. Further, the authors reported that the levels in the cornea after episcleral implant administration are higher at all the time points than those predicted by diffusion alone. Hence, it was speculated that processes other than simple diffusion, most likely ocular circulation and lymphatics, lead to higher drug levels in the cornea after periocular implant administration. A similar or another unknown mechanism of convection may contribute to high drug levels in the cornea. This mechanism and a leak-back along the needle tract from the site of administration may have contributed to high corneal levels of celecoxib after subconjunctival administration of celecoxib suspension in our studies. We collected the first tissue sample at 15 minutes, unlike the 3-hour time point of Robinson et al.¹⁴ Further, the visible bleb at the site of injection disappeared in about an hour in our study. It is likely that a leak-back contributed to high drug levels in early samples. By 3 hours in the celecoxib studies, the drug levels were in the declining phase (~40% of the peak levels). The other differences between the two studies are the formulation (an implant may not have a leak-back, whereas a suspension would) and also the species (rabbit versus rat).

Model Validation for Corneal Pharmacokinetics

We tried to validate our model using data from a previous study by Ayalasomayajula and Kompella,¹² in which they used a similar dose and volume of injection of celecoxib for the

periocular administration. However, they used the SD rats, a nonpigmented strain. When our model-predicted values for pigmented BN rats were compared with the values obtained by Ayalasangayajula and Kompella, a very good correlation was observed (Fig. 2, $r = 0.99$). Thus, the corneal pharmacokinetics were similar for celecoxib between the two strains of rats (Table 1).

We further validated our corneal model with another molecule, prednisolone, reported by Tsuji et al.⁴ in rabbits. They assessed three subconjunctival doses, 2.61, 0.261, and 26.1 mg, of prednisolone. A soluble salt of prednisolone, prednisolone sodium succinate, was used in this study. We used our optimum cornea model in rats to fit the rabbit data with a 2.61-mg dose of prednisolone and then used the data with 0.261 and 26.1 mg doses for further validation of the model. Since prednisolone sodium succinate was administered as a solution, we assumed that the entire dose was immediately available at the periocular site and that there was no dissolution/release step. The data-fit to the prednisolone levels in the cornea is shown in Figure 3. It is evident that our model resulted in a very good fit for the rabbit prednisolone data and the correlation coefficient between the observed and predicted data was excellent ($r = 0.99$). We further validated this model at two other doses (0.261 and 26.1 mg). We generated the pharmacokinetic profiles at these two doses and compared the experimental and the model-predicted data. The comparisons of the two doses between the model-predicted and the experimental data are shown in Figure 3. If the slopes of the curves obtained at different doses are similar, it indicates that the model predictions and the constants calculated are independent of concentrations in the dose range examined (0.261–26.1 mg). A similar validation was made by Lee and Robinson⁵ to explain the vitreous pharmacokinetics after subconjunctival administration of prednisolone. We also found a very good correlation between the observed and the model-predicted data. Therefore, the model generated with the 2.61-mg dose was validated with the 0.261- and 26.1-mg doses. Thus, a similar model can be used to describe the corneal pharmacokinetics in both rats and rabbits after periocular administration.

Parameter Estimates for Corneal Pharmacokinetics

The parameter estimates from the modeling procedure for celecoxib and prednisolone are shown in Tables 1 and 2, respectively. For celecoxib pharmacokinetics in rats, the elimination rate constant from the cornea was $0.138 \text{ minute}^{-1}$, which is comparable to the values reported in rabbits for other small lipophilic drugs such as lidocaine, benoxinate, and proparacaine.^{23–25} Further, the model predicted a high elimination from the periocular site, which has been well-demonstrated with several drugs, including macromolecular drugs.²⁶ It is extremely difficult to estimate the precision (mean \pm SEM) of the parameter estimates in nonlinear regression modeling, unless the software provides these precisions using an algorithm. The drawback of Berkeley Madonna as software for pharmacokinetics modeling is that it does not provide the precision (mean \pm SEM) of the parameter value. However, even the software used by Lee and Robinson⁵ (Model Maker; Family Genetix, Ltd., Wallingford, UK) has the same drawback. It would be ideal to know how precisely these parameters are estimated to make any significant statistical comparisons from two different studies. However, assuming that the parameter estimates are accurate, some reasonable conclusions can be made from our modeling studies. We initially modeled the prednisolone pharmacokinetics using the Lee and Robinson⁵ values for elimination rate constant from the periocular site ($0.128 \text{ minute}^{-1}$). However, if the subconjunctival elimination rate constant is fixed at that value, a poor data fit results. Hence, instead of fixing the value of that parameter, we allowed it to float and let the software determine its estimate. The values predicted by Berkeley Madonna for the elimination rate constant from the periocular site ($0.072 \text{ minute}^{-1}$) were somewhat different from those obtained by Lee and Robinson ($0.128 \text{ minute}^{-1}$). There are two possible explanations. First, the software used is different (present

study, Berkeley Madonna; Lee and Robinson, Model Maker) and we do not know whether the integration method used is similar, as Lee and Robinson did not mention that in their study. The software algorithm as well as the hardware can contribute to the differences in the parameter estimates in modeling.²⁷ Second, for estimating the value of the subconjunctival elimination rate constant Lee and Robinson used the vitreous pharmacokinetic data of prednisolone, whereas we used the corneal pharmacokinetic data to estimate the value. When we modeled the vitreous data of prednisolone using the model of Robinson and Lee but using Berkeley Madonna software, the parameter estimates were close for the elimination from the periocular site (0.143 vs. 0.128 minute⁻¹). It is also possible that there is some missing element in obtaining similar values for parameters such as the elimination rate constant from the periocular tissue based on independent fits to corneal and vitreous concentration profiles.

In obtaining parameter estimates for the model parameters, it is essential to ensure that a global minimum is achieved in the estimation process. Even when we varied our initial values or ranges given to the software for estimating the parameters, we still obtained similar parameter estimates on curve fitting, which suggests that the parameter values are not due to reaching a local minimum, but that very likely they are the global minimum values.

Comparison between Rat and Rabbit Corneal Pharmacokinetics after Periocular Administration

We obtained parameter estimates for two different molecules in the rat and rabbit models. Even though the molecules are structurally different, they both are lipophilic. If we assume that the structural differences would not lead to a big difference in the pharmacokinetics of these two molecules after periocular administration, some conclusions and comparisons can be made between the rabbit and the rat periocular kinetics. The rate constant for elimination from the periocular site is about two times higher in the rat than in the rabbit (Table 1 versus Table 2). Other rate constants also differ between the two species. The corneal elimination is also approximately 2.7-fold higher in the rats and the absorption rate constant is several times higher. The caveat is that for the rabbit study, the authors used a salt form of the drug prednisolone. Prednisolone solubility is 0.2 mg/mL²⁸ which is approximately 20 to 100 times that of celecoxib.^{29,30} Prednisolone sodium succinate used in the study by Tsuji et al.⁴ is expected to increase the drug's solubility further to 50 to 100 mg/mL. The formulation administered in the rabbit study was thus a solution, whereas in the studies by Cheruvu et al.¹¹ and Ayalasangayajula and Kompella,¹² the formulation administered was a suspension of celecoxib. Thus, the differences in elimination from the periocular tissue could either be due to the differences in the species or differences in the formulation. It is known that the suspension form of the drug can sustain the drug levels better than the solution form. Indeed, a periocular (posterior juxtasclear) suspension of anecortave acetate (a lipophilic, very poorly water-soluble drug) has been shown to sustain drug levels for a prolonged period in preclinical studies as well as in humans.^{31,32}

Simulation of Drug Levels in the Cornea after Administration of Solution, Suspension, or Sustained-Release Formulations

We compared the experimentally observed and best-fitted cornea profile of celecoxib suspension with simulated profiles of a formulation with instantaneous dissolution (solution) and sustained-release formulation releasing drug more slowly compared to suspension. We assumed first order drug dissolution or release. The simulated data are shown in Figure 4. During the initial time points in the 12-hour simulation (Fig. 4, inset) the levels with suspension were lower than that of the solution, but at the later time points, they were slightly higher than that of the solution. However, the differences are not dramatic, possibly

because of the inclusion of a leak-back for both formulations. When we simulated the data for a period of 60 days, it can be seen that solution and suspension dosage forms behave almost in an identical manner beyond the first 12 hours; further, the drug levels with these two dosage forms decline over several orders of magnitude during the first 5-day period. However, with a sustained-release system, initial levels were lower, but the drug levels were maintained within an order of magnitude during most of the 60-day period (Fig. 4).

Model Selection for Retinal Pharmacokinetics after Periocular Administration

The retina is the target for many posterior segment disorders including diabetic retinopathy, age-related macular degeneration, and retinitis pigmentosa. In addition, the choroid is a target in some disorders, such as choroidal neovascularization associated with age-related macular degeneration. There is currently major interest in the development of transscleral drug delivery systems as a safer alternative to the intravitreal mode of administration. In most of the studies to date, the drug concentrations have been measured in the vitreous after periocular administration. The vitreous concentrations are thought to be representative of the retinal concentrations of the therapeutic agent. Only a few studies have actually evaluated the retinal tissue concentrations after periocular administration, and very few among them have determined the retinal levels after plain solution or suspension formulation of the drug.^{31–40} It is important to know the retinal pharmacokinetics of drugs, as it is the target organ for the above-mentioned disorders. Models have been developed to describe the vitreous pharmacokinetics after periocular administration. Lee and Robinson⁵ described a three-compartment model with a parallel elimination pathway to describe the pharmacokinetics of prednisolone in the vitreous after subconjunctival (periocular) administration. In a subsequent study, they proposed a simplified version of their model, to perform simulation studies to understand the kinetics of sustained drug delivery systems in the vitreous.⁴¹ No attempt has been made to model the retinal drug concentrations after periocular or even intravitreal modes of administration. We used the data of Cheruvu et al.,¹¹ and developed a model describing the pharmacokinetics of drugs in the retina after periocular administration. As described in the corneal model's development, we started with the simplest model wherein the drug directly penetrates the retina after periocular administration. The absorption constant for the retina is a hybrid of the absorption across the sclera–choroid and the RPE. This model is similar to the simple vitreous model proposed by Lee and Robinson.⁴¹ The data from the retinal celecoxib concentrations in BN rats were fitted to this model by using the curve-fitting procedure. The data-fits are shown in the Figure 5A. As can be seen, data at several time points were not fit well by the model (R^2 : 0.65; AIC: 260), and the fits can definitely be improved. By evaluating the terminal (elimination) phase in the retinal kinetics of celecoxib, it can be seen that the drug follows multiphasic disposition from the retina. To model this, we included a distribution compartment into which the drug was distributed from the retina. This distribution compartment could be a combination of vitreous and probably the lens in the rat. However, inclusion of this distribution compartment did not lead to any significant improvement in the data-fits (Fig. 5B; R^2 : 0.63; AIC: 263.3). One important observation is that in both cases, the C_{\max} was not well fit, and the t_{\max} was achieved later than the model predicted. These findings indicate a lag phase in the kinetic profile. Since the formulation used was a suspension, a dissolution step is required before the drug becomes available for absorption. This process of dissolution/release may explain the greater than predicted t_{\max} . We modified the model to include the dissolution step. With the revised model without a distribution compartment associated with retina, the t_{\max} predicted by the model and the actually observed t_{\max} were quite close (Fig. 5C) and the fit was better (R^2 : 0.86; AIC: 231.3). However, the last few data points were underpredicted by the model, suggesting the existence of a distribution compartment. When the distribution compartment was added to

the retina, the fits improved significantly and the model-predicted values fit well to the observed concentrations at all the time points (R^2 : 0.9; AIC: 223.3; Fig. 5 D).

Figures 5C and 5D show that the C_{\max} was slightly under-predicted by the model. We considered two more types of models to improve the C_{\max} prediction. The drug has to cross the sclera and the choroid-RPE to reach the retina after periocular administration. In this process, there is a possibility that some of the drug is eliminated by the episcleral and choroidal circulation and lymphatics. Hence, instead of using a hybrid rate constant for absorption (which combines absorption in sclera, choroid, and retina) an inclusion of a transfer compartment that could be either the choroid or a combination of the sclera-choroid-RPE may lead to a better fit. Further, since the drug can be eliminated from the sclera-choroid-RPE (transfer compartment/choroidal compartment), we used a third parallel elimination pathway from the choroid. The structural model is shown in Figure 5E. When the data were fit to this revised model, an excellent data-fit was obtained (R^2 : 0.92; AIC: 218.4). All the time points were well fit by this model. Further, this model predicted the C_{\max} better than the previous models. There was good correlation between the observed and the model-predicted data. We included a distribution compartment for the choroidal compartment, to evaluate whether this would further improve the goodness of fit. However, no further improvement was achieved by inclusion of this compartment (data not shown). Thus, the model in Figure 5E was initially selected as the model to describe retinal pharmacokinetics after periocular administration. The elimination from the retina could be due to retinal blood flow or metabolism of the drug in the retina. There is not much evidence that a significant drug metabolism can take place in the neural retina. The RPE has metabolic activity, but we have included the RPE as a part of the transfer compartment, as the retinal concentrations measured in the studies are concentrations in the neural retina. Also, the blood flow to the choroid is significantly greater than the blood flow to the retina in many species including the rat, rabbit, cat, and the dog.⁴²⁻⁴⁵ In addition, the choroidal vessels are leakier and the choroidal vessels perform much of the retinal perfusion in mammals. It has been demonstrated by cryotherapy that choroidal blood flow does not play a significant role in the removal of triamcinolone acetonide after periocular administration.¹⁴ It has been argued that cryotherapy does not cause damage to the episcleral and conjunctival circulation but does affect the choroidal circulation. However, no actual measurements have been made of the choroidal and conjunctival blood flow with and without the cryotherapy. Also, only one time point was evaluated, and no statistical comparisons were performed. It is possible that the drug is eliminated via the choroid even when given intravitreally.^{46,47} Several previous modeling attempts have used the choroid as a perfect sink and have good fit between the model-predicted and observed data for intravitreal kinetics.⁴⁸⁻⁵¹ Hence, we evaluated an additional model that did not have elimination from the retina. We assumed that the drug is distributed from the choroidal compartment (transfer compartment) into the retina but is eliminated primarily through the choroidal compartment and the periocular tissue. The fits to the revised model are shown in Figure 5F. The difference between Figures 5E and 5F is the presence or absence of the retinal elimination pathway, respectively. The model in Figure 5E (R^2 : 0.92; AIC: 218.4) with an elimination pathway in the retina results in a better fit than the model in Figure 5F (R^2 : 0.89; AIC: 228). There are species differences in the retinal circulation, with humans and rodents having a holangioretinal retina and rabbits having a merangioretinal retina.^{52,53} The model in Figure 5F without the retinal elimination pathway may be more representative of the rabbit physiology. Based on the statistical goodness-of-fit criteria model described in Figure 5E was selected as the finalized model to describe retinal pharmacokinetics after periocular administration in the rat model.

Most of our retina models underpredicted C_{\max} . One potential explanation is that there is a systemic recirculation component contributing to retinal drug levels. We included such a possibility in the models to improve the prediction of C_{\max} and to enhance the overall data-

fit. We considered four recirculation models, which are essentially those shown in Figures 5C–F, but with the addition of a systemic circulation compartment that communicates with the vascularized tissues in the back of the eye and eliminates the drug from the system (Fig. 6). None of the recirculation models evaluated resulted in a better fit to the data than the models described herein (Fig. 6). Also, the predicted C_{\max} values with the recirculation models were not as good as those predicted by the model in Figure 5E. Hence, the model in Figure 5E was selected as the final model. We validated the model in Figure 5E using the retinal pharmacokinetics data in nonpigmented SD rats. The model resulted in an excellent fit to the observed data ($r=0.99$; Fig. 7). Thus, a similar model can be used to describe the pharmacokinetics of celecoxib in the pigmented and nonpigmented rat retina although the parameter estimates can differ.

Parameter Estimates for Retinal Pharmacokinetics of Celecoxib after Periocular Administration

As discussed in the section on corneal pharmacokinetics modeling, we found that fitting different data sets (corneal or vitreous data after periocular administration of prednisolone to rabbits) gave different values for the elimination rate constant from the periocular space (0.072 vs. 0.143 minute^{-1}), therefore in our retinal modeling, we did not fix the value of the periocular elimination rate constant. However, the values obtained for the elimination rate constant for celecoxib from the periocular tissue from either the corneal or retinal pharmacokinetics data of celecoxib were very close (0.123 minute^{-1} with retinal data versus 0.135 minute^{-1} with corneal data). The estimates for the other parameters are shown in Table 3. The parameter estimates indicate that the elimination rate constant of celecoxib from the periocular site was approximately threefold greater than its elimination from the choroidal compartment (transfer compartment; 0.123 vs. 0.035 minute^{-1}). Further, the choroidal elimination rate constant for celecoxib was 18-fold greater than the retinal elimination rate constant (0.035 vs. 0.002 minute^{-1}). Using animal models, Robinson et al.¹⁴ showed that the conjunctival circulation and lymphatics play a much greater role in the elimination of drugs after periocular administration compared with the clearance by the choroidal circulation. This route is even believed to be responsible for the clearance of macromolecules from the periocular site, as was shown in the case of albumin by Bill,^{54,55} who demonstrated that the albumin is eliminated partly by the conjunctival circulation and lymphatics. We also found that the conjunctival circulation and lymphatics could be playing a role in the clearance of small (20 nm) nanoparticles.⁵⁶ Also Liu et al.⁵⁷ demonstrated that the conjunctival lymphatics play a role in clearing latex particles, ultimately leading to accumulation of the latex particles in the cervical lymph nodes after subconjunctival administration.

The absorption rate constant for absorption into the choroidal compartment (transfer compartment) is lower than the absorption from the transfer compartment into the retina (Table 3). This means that the absorption into the transfer compartment is a rate-limiting step in the availability of the drugs to the retina after periocular administration. In the recent past, we demonstrated in transport studies in vitro that the choroid is a significant anatomic barrier to the transport of drugs and that the barrier properties or resistances increase with increasing lipophilicity of the drugs.⁵⁸ Similarly, others have demonstrated that the RPE is a significant barrier to the transscleral delivery of drugs to the retina, and the resistance of the RPE is higher to hydrophilic drugs than to lipophilic drugs.⁵⁹ However, our model suggests that if the drug or delivery system is directly injected into the transfer compartment, the retinal availability would significantly increase, because a significant portion of the elimination by the subconjunctival and episcleral circulations can be avoided. Recently, Kim et al.¹⁵ using MRI, demonstrated that periocular administration does not lead to significant drug levels in the posterior segment intraocular tissues; however, if the drug is administered

by an intrascleral infusion, significant drug levels can be seen in the posterior intraocular tissues. We used the finalized model (Fig. 5E) to fit the celecoxib retinal pharmacokinetics data in nonpigmented rats. Very good data fits were obtained and there was a good correlation between the predicted and observed values (Fig. 6). The predicted parameter estimates for the nonpigmented rats are shown in Table 3. The elimination rate constant from the periocular space appeared to be similar between the BN and SD rats (0.123 vs. 0.115 minute^{-1}). All other parameters were also similar, with the only major differences being in the parameter K30 (elimination rate constant from the retina), which was approximately 100-fold greater in the BN rats than in the SD rats (Table 3). We also observed that the dissolution/release rate constant for celecoxib is similar based on corneal data as well as retinal data in both the rat strains (Tables 1, 3). As discussed in the section on corneal modeling, the precision of the parameter estimates is not known, and hence no conclusive statement can be made about the statistical significance of these differences. With more data and use of software programs with built-in features for calculating the precisions, this problem can be solved. We tried to use another pharmacokinetic modeling software (WinNonlin 1.5; Pharsight Corp., Mountain View, CA) in our modeling, because it provides precision of the parameter estimates. However, the software algorithm failed to converge with some of the modeling strategies in the present analysis. It has been shown that there are significant differences in retinal AUC of celecoxib after periocular administration to BN and SD rats, with the levels being higher in SD rats than in the BN rats. From the parameter estimates in the two species, we cannot determine which parameter influenced this difference in the retinal AUCs. It could be a single parameter or a combination that leads to the observed differences. The binding of the drug to melanin can be included in each of the modeling compartments where melanin is present. To keep the approach simple and to minimize the number of parameters, we did not include this component in our modeling strategy.

Thus, the retinal kinetics can be described by a four-compartment model after periocular administration. The conjunctival, episcleral, and choroidal circulation play a significant role in the clearance of the drugs from the retina after periocular administration. Entry or accumulation into transfer compartment appears more rate limiting than entry into neural retina. A similar model describes the pharmacokinetics in the retina after periocular administration in both pigmented and nonpigmented rats, but the parameter estimates differ.

Simulation of Drug Levels in the Retina after Administration of Solution, Suspension, or Sustained-Release Formulations

We also performed simulations after the administration of three different hypothetical formulations, as described under corneal pharmacokinetics. The difference between the solution and suspension dosage form kinetics is more striking with respect to the retinal levels when compared with the cornea. During the short 12-hour simulation with the solution and suspension dosage forms, it can be seen that the solution dosage form had a high C_{max} and a lower t_{max} . The suspension dosage form had a lower C_{max} but it sustained the drug levels better than the solution dosage form (Fig. 8, inset). During the longer-term simulation over a 60-day period with the three different formulations, similar to the cornea, the sustained-release dosage form maintained the drug levels in the retina within 1 order of magnitude for most of the 60-day period. With the solution and suspension dosage forms, on the other hand, there was a rapid initial decline followed by a gradual decline in the drug levels over several orders of magnitude (Fig. 8). Thus, it can be inferred from the model simulations that solution and suspension dosage forms of celecoxib do not sustain significant levels of drugs in the cornea or retina for a prolonged period. However, with a sustained-release system releasing drug at a much slower rate, tissue levels can be maintained for prolonged periods.

Conclusions

Retinal and corneal pharmacokinetics of drugs after periocular administration are still emerging. The reported data are sparse to none in the rodents (rat and mice), the animal models that are widely used in efficacy assessment. In this study, we developed and validated readily usable compartment models to explain the retinal and corneal levels of small lipophilic drugs after periocular subconjunctival administration. The modeling studies indicated that retinal pharmacokinetics can be explained with a four-compartment model that incorporates primary elimination pathways from the choroid region and retina, as well as a periocular site. The drug elimination rate constant was threefold higher from the periocular space than from the choroid region. Similar models can be used to explain retinal pharmacokinetics in the pigmented and nonpigmented rats. The two rat strains did not differ in their periocular elimination rate constants. While some other parameters differed, their physiological significance should be assessed with experiments in future studies.

Further, our studies indicate that the corneal pharmacokinetics after periocular administration can be explained with similar models in rats and rabbits. The elimination rate constants from the periocular space and the cornea are of a similar order of magnitude between the rats and rabbits for two different lipophilic molecules. However, the rate constant was lower in rabbits. The difference could be due to the drug or species—which one must be ascertained in future studies.

Whereas the periocular route in this study referred to the subconjunctival or posterior subconjunctival region, future studies investigating multiple periocular routes are expected to result in more site-dependent pharmacokinetic information. Although, noninvasive fluorophotometry with the Fluorotron Master (Ocumetrics, Mountain View, CA)–based quantification is emerging as a method of determining vitreous levels after various periocular routes of administration,⁶⁰ data on drug quantification in the retina are sparse. We are currently establishing the reliability of Fluorotron measurements for pharmacokinetics analysis. Although Fluorotron allows the measurement of only fluorescein and related fluorophores, other noninvasive techniques such as magnetic resonance imaging assess only the disposition of contrast agents or contrast agent–labeled solutes, which may not be truly reflective of the solute's disposition. For any modeling study, tissue data should be analyzed by using reliable analytical methods such as HPLC analysis, as was the case with the data used in this study. In future, more such data will enable better mathematical modeling of the pharmacokinetics of drugs in various layers of the posterior eye after periocular administration.

Acknowledgments

Supported by an unrestricted research gift from Pfizer Global Research and by National Eye Institute Grants R24 EY017045, R01 DK064172, R03 EY013842, and R21 EY017360.

References

1. Maurice DM. Drug delivery to the posterior segment from drops. *Surv Ophthalmol.* 2002; 47(suppl 1):S41–S52. [PubMed: 12204700]
2. Raghava S, Hammond M, Kompella UB. Periocular routes for retinal drug delivery. *Expert Opin Drug Deliv.* 2004; 1:99–114. [PubMed: 16296723]
3. Ranta VP, Urtti A. Transscleral drug delivery to the posterior eye: prospects of pharmacokinetic modeling. *Adv Drug Deliv Rev.* 2006; 58:1164–1181. [PubMed: 17069929]
4. Tsuji A, Tamai I, Sasaki K. Intraocular penetration kinetics of prednisolone after subconjunctival injection in rabbits. *Ophthalmic Res.* 1988; 20:31–43. [PubMed: 3380524]

5. Lee TW, Robinson JR. Drug delivery to the posterior segment of the eye II: development and validation of a simple pharmacokinetic model for subconjunctival injection. *J Ocul Pharmacol Ther.* 2004; 20:43–53. [PubMed: 15006158]
6. Weijtens O, Feron EJ, Schoemaker RC, et al. High concentration of dexamethasone in aqueous and vitreous after subconjunctival injection. *Am J Ophthalmol.* 1999; 128:192–197. [PubMed: 10458175]
7. Rootman J, Ostry A, Gudauskas G. Pharmacokinetics and metabolism of 5-fluorouracil following subconjunctival versus intravenous administration. *Can J Ophthalmol.* 1984; 19:187–191. [PubMed: 6744104]
8. Souli M, Kopsinis G, Kavouklis E, Gabriel L, Giamarellou H. Vancomycin levels in human aqueous humour after intravenous and subconjunctival administration. *Int J Antimicrob Agents.* 2001; 18:239–243. [PubMed: 11673036]
9. Rowland, M.; Balant, L.; Peck, C. AAPS PharmSci; Physiologically based pharmacokinetics in drug development and regulatory science: a workshop report; Georgetown University, Washington, DC. May 29–30, 2002; 2004. p. E6
10. Loizou GD, Spendiff M. A human PBPK model for ethanol describing inhibition of gastric motility. *J Mol Histol.* 2004; 35:687–696. [PubMed: 15614624]
11. Cheruvu NP, Amrite AC, Kompella UB. Effect of eye pigmentation on trans-scleral drug delivery. *Invest Ophthalmol Vis Sci.* In press.
12. Ayalasmayajula SP, Kompella UB. Retinal delivery of celecoxib is several-fold higher following subconjunctival administration compared to systemic administration. *Pharm Res.* 2004; 21:1797–1804. [PubMed: 15553225]
13. Li SK, Molokhia SA, Jeong EK. Assessment of subconjunctival delivery with model ionic permeants and magnetic resonance imaging. *Pharm Res.* 2004; 21:2175–2184. [PubMed: 15648248]
14. Robinson MR, Lee SS, Kim H, et al. A rabbit model for assessing the ocular barriers to the transscleral delivery of triamcinolone acetonide. *Exp Eye Res.* 2006; 82:479–487. [PubMed: 16168412]
15. Kim SH, Galban CJ, Lutz RJ, et al. Assessment of subconjunctival and intrascleral drug delivery to the posterior segment using dynamic contrast-enhanced magnetic resonance imaging. *Invest Ophthalmol Vis Sci.* 2007; 48:808–814. [PubMed: 17251481]
16. Makoid MC, Robinson JR. Pharmacokinetics of topically applied pilocarpine in the albino rabbit eye. *J Pharm Sci.* 1979; 68:435–443. [PubMed: 438963]
17. Maurice, DM.; Mishima, S. Ocular pharmacokinetics.. In: Sears, ML., editor. *Pharmacology of the Eye.* Springer; New York: 1984. p. 19-116.
18. Sasaki H, Kashiwagi S, Mukai T, et al. Topical delivery system of ophthalmic drugs by periocular injection with viscous solution. *Biol Pharm Bull.* 1999; 22:961–965. [PubMed: 10513621]
19. Sasaki H, Kashiwagi S, Mukai T, et al. Drug absorption behavior after periocular injections. *Biol Pharm Bull.* 1999; 22:956–960. [PubMed: 10513620]
20. Wine NA, Gornall AG, Basu PK. The ocular uptake of subconjunctivally injected 14C-hydrocortisone. *Am J Ophthalmol.* 1964; 58:362–366. [PubMed: 14204798]
21. Kim H, Csaky KG, Gilger BC, et al. Preclinical evaluation of a novel episcleral cyclosporine implant for ocular graft-versus-host disease. *Invest Ophthalmol Vis Sci.* 2005; 46:655–662. [PubMed: 15671296]
22. Lee SS, Kim H, Wang NS, et al. A pharmacokinetic and safety evaluation of an episcleral cyclosporine implant for potential use in high-risk keratoplasty rejection. *Invest Ophthalmol Vis Sci.* 2007; 48:2023–2029. [PubMed: 17460256]
23. Levy JH. Intraocular sporotrichosis. Report of a case. *Arch Ophthalmol.* 1971; 85:574–579. [PubMed: 5087599]
24. Smolen VF, Siegel FP. Procaine interaction with the corneal surface and its relation to anesthesia. *J Pharm Sci.* 1967; 57:378–384. [PubMed: 5655574]
25. Polse KA, Keener RJ, Jauregui MJ. Dose-response effects of corneal anesthetics. *Am J Optom Physiol Opt.* 1978; 55:8–14. [PubMed: 677245]

26. Hoffmann F, Zhang EP, Mueller A, et al. Contribution of lymphatic drainage system in corneal allograft rejection in mice. *Graefes Arch Clin Exp Ophthalmol*. 2001; 239:850–858. [PubMed: 11789866]
27. Bonate, PL. *The Art of Modeling: Pharmacokinetic-Pharmacodynamic Modeling and Simulation*. Springer Science and Business Media Inc; New York: 2006. p. 1-56.
28. Zhao L, Orton E, Vemuri NM. Predicting solubility in multiple nonpolar drugs-cyclodextrin system. *J Pharm Sci*. 2002; 91:2301–2306. [PubMed: 12379915]
29. Garti N, Avrahami M, Aserin A. Improved solubilization of Celecoxib in U-type nonionic microemulsions and their structural transitions with progressive aqueous dilution. *J Colloid Interface Sci*. 2006; 299:352–365. [PubMed: 16529763]
30. Seedher N, Bhatia S. Solubility enhancement of Cox-2 inhibitors using various solvent systems. *AAPS PharmSciTech*. 2003; 4:E33. [PubMed: 14621965]
31. Dahlin DC, Rahimy MH. Pharmacokinetics and metabolism of anecortave acetate in animals and humans. *Surv Ophthalmol*. 2007; 52(suppl 1):S49–S61. [PubMed: 17240257]
32. Kaiser PK, Goldberg MF, Davis AA. Posterior juxtasclear depot administration of anecortave acetate. *Surv Ophthalmol*. 2007; 52(suppl 1):S62–S69. [PubMed: 17240258]
33. Saishin Y, Silva RL, Saishin Y, et al. Periocular injection of micro-spheres containing PKC412 inhibits choroidal neovascularization in a porcine model. *Invest Ophthalmol Vis Sci*. 2003; 44:4989–4993. [PubMed: 14578426]
34. Okabe K, Kimura H, Okabe J, et al. Effect of benzalkonium chlo-ride on transscleral drug delivery. *Invest Ophthalmol Vis Sci*. 2005; 46:703–708. [PubMed: 15671302]
35. Hayden BC, Jockovich ME, Murray TG, et al. Pharmacokinetics of systemic versus focal Carboplatin chemotherapy in the rabbit eye: possible implication in the treatment of retinoblastoma. *Invest Ophthalmol Vis Sci*. 2004; 45:3644–3649. [PubMed: 15452072]
36. Amrite AC, Ayalasomayajula SP, Cheruvu NP, Kompella UB. Single periocular injection of celecoxib-PLGA microparticles inhibits diabetes-induced elevations in retinal PGE2, VEGF, and vascular leakage. *Invest Ophthalmol Vis Sci*. 2006; 47:1149–1160. [PubMed: 16505053]
37. Ayalasomayajula SP, Kompella UB. Subconjunctivally administered celecoxib-PLGA microparticles sustain retinal drug levels and alleviate diabetes-induced oxidative stress in a rat model. *Eur J Pharmacol*. 2005; 511:191–198. [PubMed: 15792788]
38. Kompella UB, Bandi N, Ayalasomayajula SP. Subconjunctival nanoand microparticles sustain retinal delivery of budesonide, a corticosteroid capable of inhibiting VEGF expression. *Invest Ophthalmol Vis Sci*. 2003; 44:1192–1201. [PubMed: 12601049]
39. Bodker FS, Ticho BH, Feist RM, Lam TT. Intraocular dexamethasone penetration via subconjunctival or retrobulbar injections in rabbits. *Ophthalmic Surg*. 1993; 24:453–457. [PubMed: 8351091]
40. Yanagi Y, Tamaki Y, Obata R, et al. Subconjunctival administration of bucillamine suppresses choroidal neovascularization in rat. *Invest Ophthalmol Vis Sci*. 2002; 43:3495–3499. [PubMed: 12407161]
41. Lee TW, Robinson JR. Drug delivery to the posterior segment of the eye III: the effect of parallel elimination pathway on the vitreous drug level after subconjunctival injection. *J Ocul Pharmacol Ther*. 2004; 20:55–64. [PubMed: 15006159]
42. Alm A, Bill A. The oxygen supply to the retina. 2. Effects of high intraocular pressure and of increased arterial carbon dioxide tension on uveal and retinal blood flow in cats. A study with labelled microspheres including flow determination in brain and other tissues. *Acta Physiol Scand*. 1972; 84:306–319. [PubMed: 4553229]
43. Friedman E, Kopald HH, Smith TR. Retinal and choroidal blood flow determined with Krypton-85 anesthetized animals. *Invest Ophthalmol*. 1964; 3:539–547. [PubMed: 14229941]
44. Stefansson E, Wagner HG, Seida M. Retinal blood flow and its autoregulation measured by intraocular hydrogen clearance. *Exp Eye Res*. 1988; 47:669–678. [PubMed: 3197768]
45. Yu DY, Alder VA, Cringle SJ. Measurement of blood flow in rat eyes by hydrogen clearance. *Am J Physiol*. 1991; 261:H960–H968. [PubMed: 1887939]
46. Moseley H, Foulds WS. The movement of xenon-133 from the vitreous to the choroid. *Exp Eye Res*. 1982; 34:169–179. [PubMed: 7060645]

47. Moseley H, Foulds WS, Allan D, Kyle PM. Routes of clearance of radioactive water from the rabbit vitreous. *Br J Ophthalmol*. 1984; 68:145–151. [PubMed: 6696868]
48. Kim H, Robinson MR, Lizak MJ, et al. Controlled drug release from an ocular implant: an evaluation using dynamic three-dimensional magnetic resonance imaging. *Invest Ophthalmol Vis Sci*. 2004; 45:2722–2731. [PubMed: 15277497]
49. Park J, Bungay PM, Lutz RJ, et al. Evaluation of coupled convective-diffusive transport of drugs administered by intravitreal injection and controlled release implant. *J Control Release*. 2005; 105:279–295. [PubMed: 15896868]
50. Missel PJ. Finite and infinitesimal representations of the vasculature: ocular drug clearance by vascular and hydraulic effects. *Ann Biomed Eng*. 2002; 30:1128–1139. [PubMed: 12502224]
51. Missel PJ. Hydraulic flow and vascular clearance influences on intravitreal drug delivery. *Pharm Res*. 2002; 19:1636–47. [PubMed: 12458669]
52. De Schaepdrijver L, Simoens P, Lauwers H, De Geest JP. Retinal vascular patterns in domestic animals. *Res Vet Sci*. 1989; 47:34–42. [PubMed: 2772405]
53. Germer A, Biedermann B, Wolburg H, et al. Distribution of mitochondria within Muller cells, I. Correlation with retinal vascularization in different mammalian species. *J Neurocytol*. 1998; 27:329–345. [PubMed: 9923979]
54. Bill A. Movement of albumin and dextran through the sclera. *Arch Ophthalmol*. 1965; 74:248–252. [PubMed: 14318504]
55. Bill A. Capillary permeability to and extravascular dynamics of myoglobin, albumin and gammaglobulin in the uvea. *Acta Physiol Scand*. 1968; 73:511–522. [PubMed: 4179191]
56. Amrite AC, Kompella UB. Size-dependent disposition of nanoparticles and microparticles following subconjunctival administration. *J Pharm Pharmacol*. 2005; 57:1555–1563. [PubMed: 16354399]
57. Liu H, Meagher CK, Moore CP, Phillips TE. M cells in the follicle-associated epithelium of the rabbit conjunctiva preferentially bind and translocate latex beads. *Invest Ophthalmol Vis Sci*. 2005; 46:4217–4223. [PubMed: 16249501]
58. Cheruvu NP, Kompella UB. Bovine and porcine transscleral solute transport: influence of lipophilicity and the choroid-Bruch's layer. *Invest Ophthalmol Vis Sci*. 2006; 47:4513–4522. [PubMed: 17003447]
59. Pitkanen L, Ranta VP, Moilanen H, Urtti A. Permeability of retinal pigment epithelium: effects of permeant molecular weight and lipophilicity. *Invest Ophthalmol Vis Sci*. 2005; 46:641–646. [PubMed: 15671294]
60. Ghate D, Brooks W, McCarey BE, Edelhauser HF. Pharmacokinetics of intraocular drug delivery by periocular injections using ocular fluorophotometry. *Invest Ophthalmol Vis Sci*. 2007; 48:2230–2237. [PubMed: 17460284]

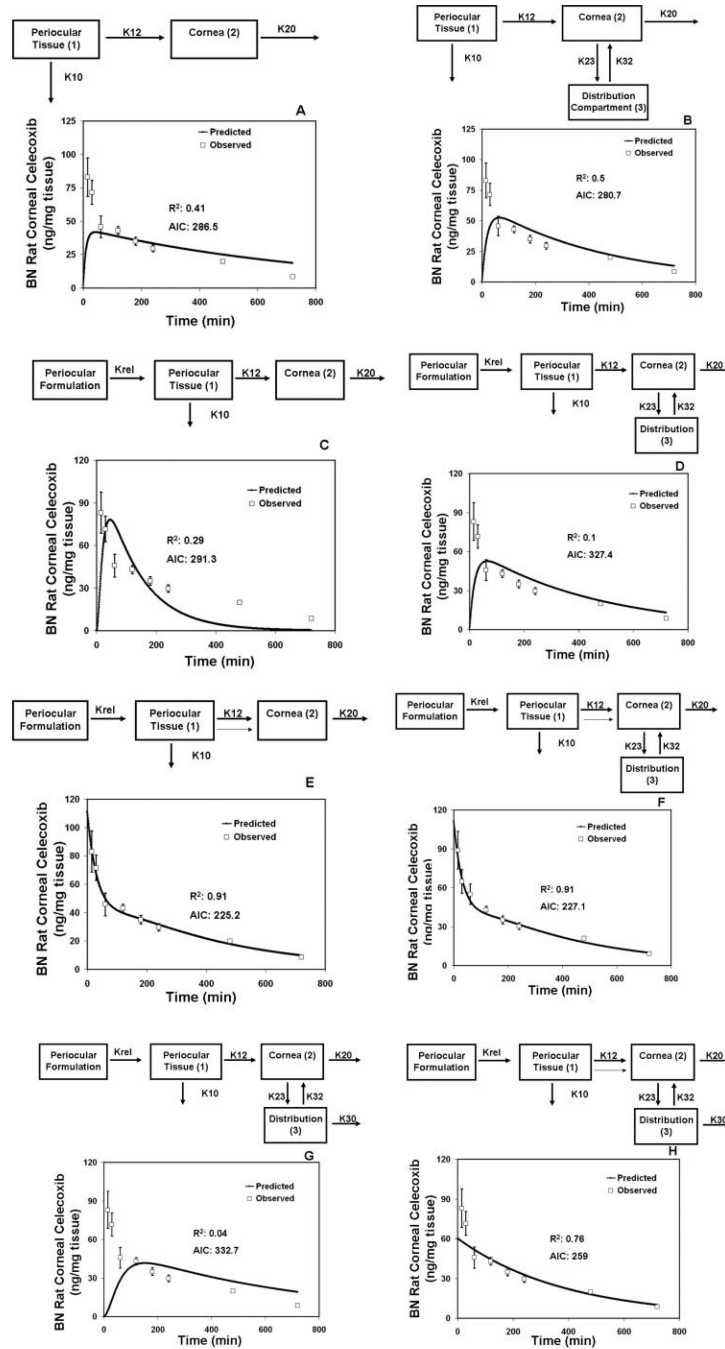


Figure 1. Model-predicted and observed concentrations of celecoxib in the cornea after administration of 3 mg celecoxib by periocular injection to BN rats. **(A)** Two-compartment model. **(B)** Three-compartment model with a distribution compartment for the cornea. **(C)** Three-compartment model with a dissolution step included for the suspension formulations. **(D)** Four-compartment model with a distribution compartment for the cornea, and a dissolution/release step included for the suspension formulation. **(E)** Three-compartment model with a dissolution/release step for suspension formulation and initial value in the cornea estimated as a parameter. *Lighter arrow*: leak-back to the cornea from the site of administration after

periocular injection. **(F)** Four-compartment model with a distribution compartment for the cornea, dissolution/release step for the suspension formulation, and initial concentration in the cornea estimated as a separate parameter. *Lighter arrow*: leak-back to the cornea. **(G)** Four-compartment model with a distribution compartment for the cornea, dissolution/release step for the formulation, and elimination from the distribution compartment. **(H)** Four-compartment model with a distribution compartment for the cornea, dissolution/release step for the formulation, and elimination from the distribution compartment and the initial concentration in the cornea estimated as a separate parameter. *Lighter arrow*: leak-back to the cornea. The model in **(E)** was selected as the finalized model. K10, elimination rate constant from the periocular site; K12, absorption rate constant for the cornea; K20, elimination rate constant from the cornea; K23, rate constant for transfer of drug from the cornea to the distribution compartment; K32, rate constant for transfer of drug from the distribution compartment to the cornea; K30, elimination rate constant from the distribution compartment; Krel, release/dissolution rate constant for the dissolution of the drug from the formulation. The observed data are expressed as the mean \pm SD for $n = 4$.

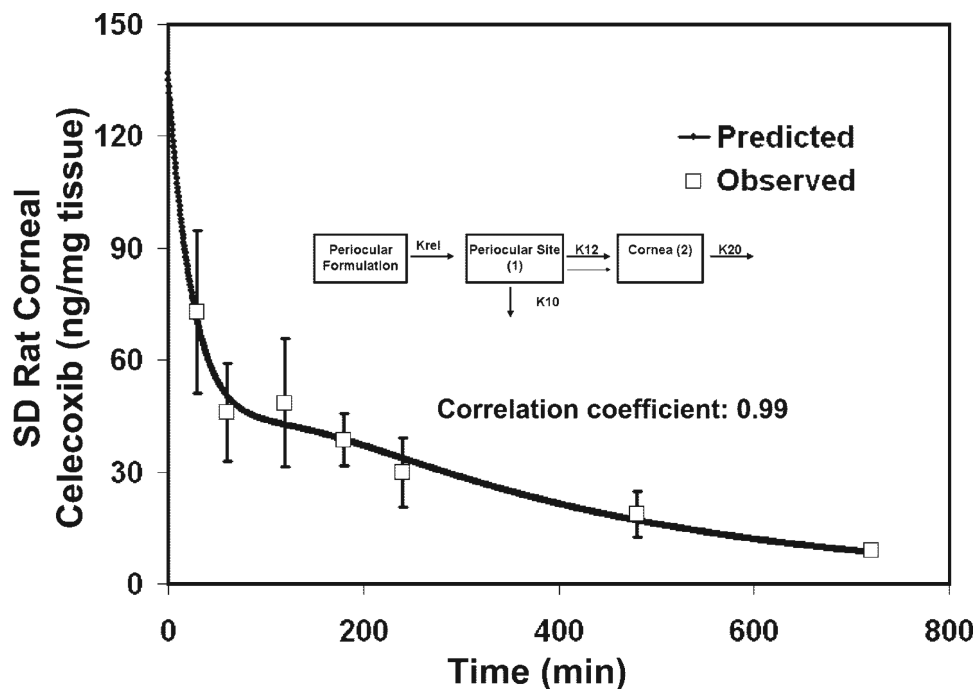


Figure 2. Validation of the corneal pharmacokinetics model described in Figure 1E by using the data of Ayalasmayajula and Kompella for celecoxib periocular administration in SD rats. *Inset:* finalized structural model developed from using the celecoxib pharmacokinetics data in BN rats by Cheruvu et al.¹¹ The data predicted from the finalized model was compared to the data obtained by Ayalasmayajula et al.¹² A very good correlation was obtained between the model-predicted and experimentally observed values. The observed data are expressed as the mean \pm SD for $n = 3$.

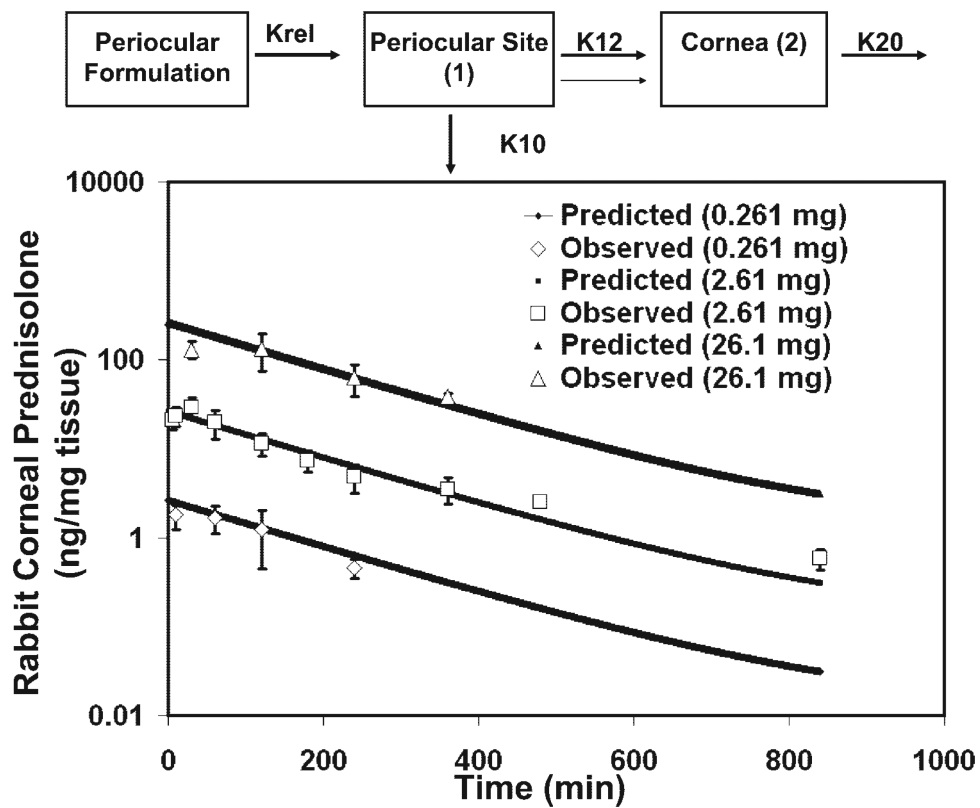


Figure 3. Validation of the corneal pharmacokinetics model described in Figure 4 by using the data of Tsuji et al.⁴ for subconjunctival administration of prednisolone in rabbits. The prednisolone data was fit to the model by curve fitting. The observed data are expressed as the mean \pm SEM for $n = 3-9$. Excellent correlation was found between the observed and the model-predicted data.

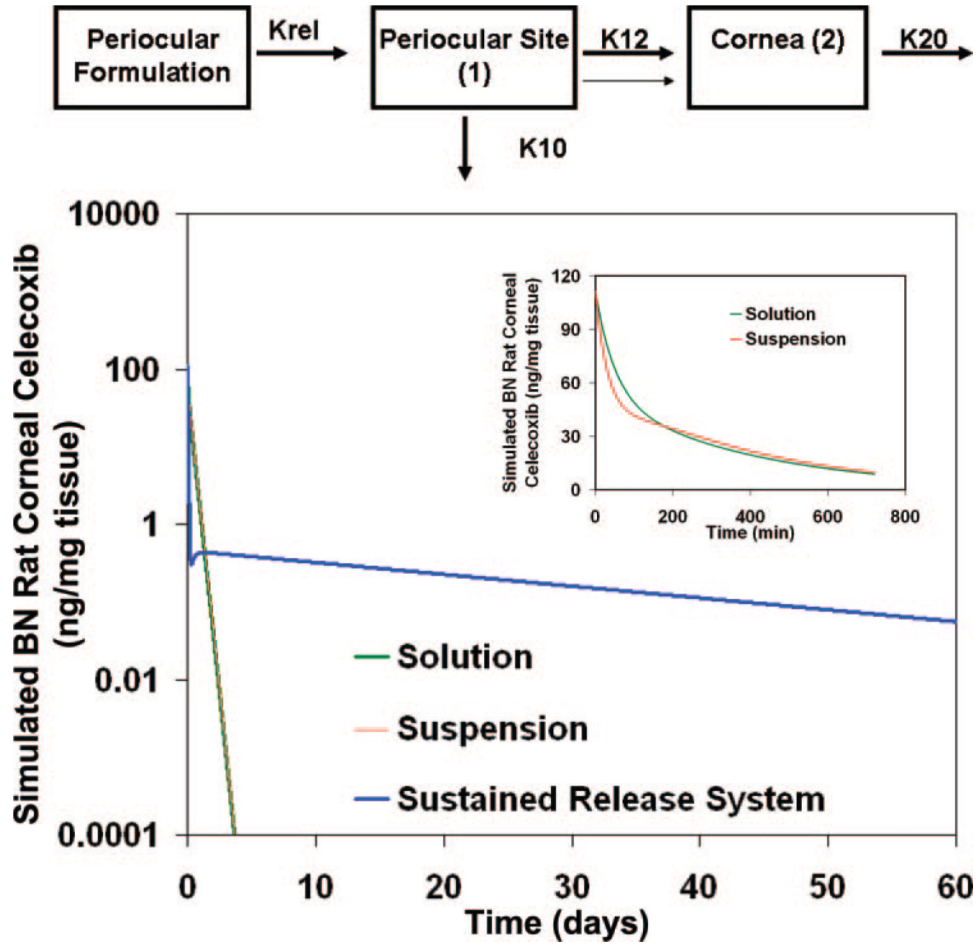


Figure 4. Simulation of celecoxib drug levels in the cornea of BN rats by using the parameter estimates in Table 1 and the model in Figure 1E, after administration of 3 mg celecoxib by the periocular route as a solution, suspension, or sustained-release system. The sustained-release system was assumed to have a release rate 1000 times less than the release from suspension. *Top:* structural model; *inset:* simulated corneal levels of celecoxib during the initial 12 hours after solution and suspension administration.

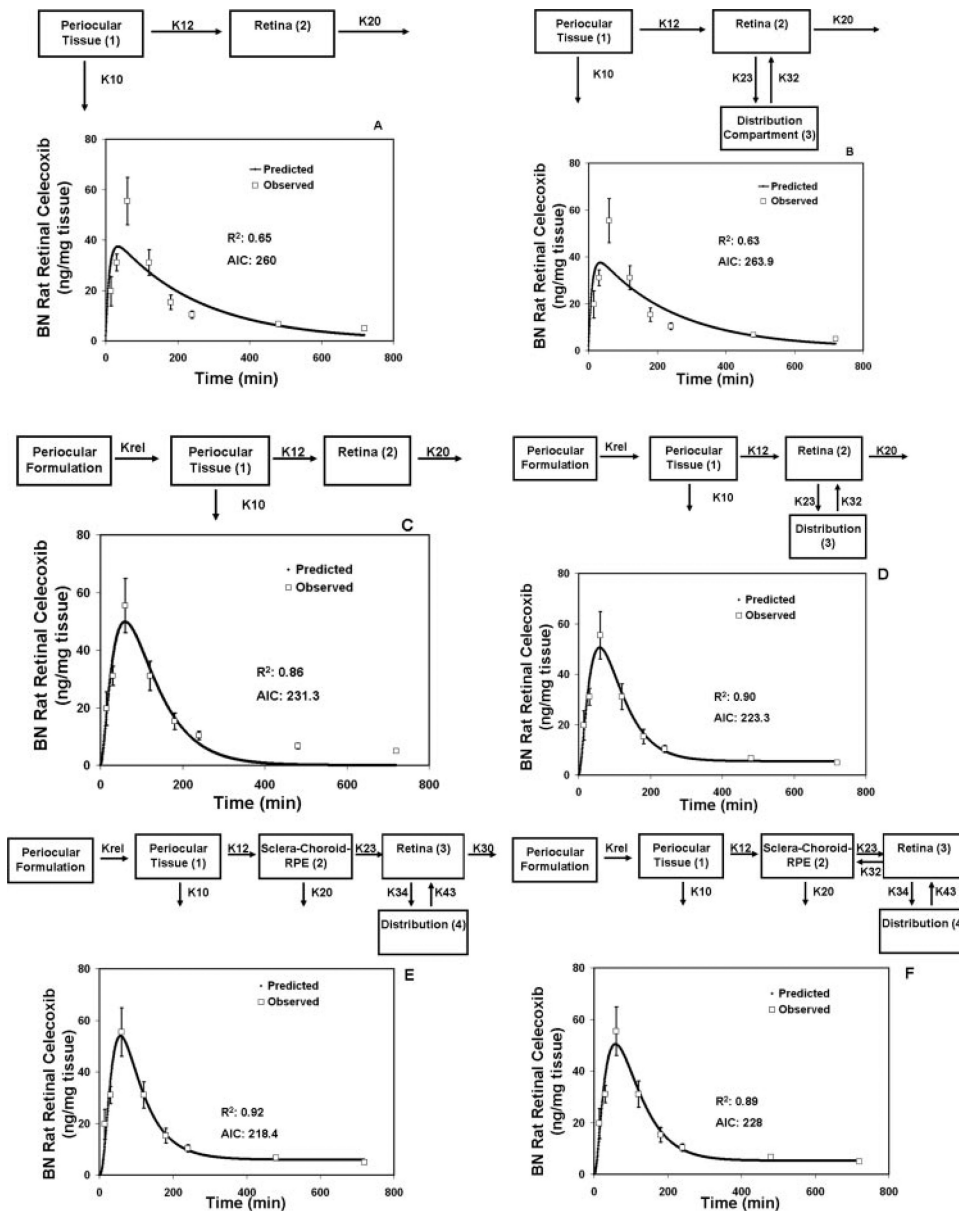


Figure 5. Model-predicted and observed concentrations of celecoxib in the retina after administration of 3 mg celecoxib by periocular injection to BN rats. **(A)** Two-compartment model. **(B)** Three-compartment model with a distribution compartment to the retina. **(C)** Three-compartment model with a dissolution/release step included for the suspension formulations. **(D)** Four-compartment model with a distribution compartment for the retina and a dissolution/release step included for the suspension formulation. **(E)** Five-compartment model with a transfer compartment representing the sclera-choroid-RPE, a distribution compartment to the retina and a dissolution/release step included for the suspension formulation. **(F)** Five-compartment model with a transfer compartment representing the sclera-choroid-RPE, a distribution compartment to the retina, no retinal elimination and a dissolution/release step included for the suspension formulation. The model in **(E)** was selected as the finalized model to describe retinal pharmacokinetics after periocular administration. **(A–D)** K10, elimination rate constant from the periocular tissue; K12,

absorption rate constant for the retina; K20, elimination rate constant for the retina; K23, rate constant for transfer of drug from the retina into the distribution compartment; K32, rate constant for transfer of drug from the distribution compartment to the retina; Krel, rate constant for dissolution/release of celecoxib from the formulation. (E, F) K10, elimination rate constant for periocular site; K12, absorption rate constant for sclerachoroid-RPE (transfer compartment). K20, elimination rate constant for sclera-choroid-RPE; K23, transfer constant to the retina from the sclerachoroid-RPE; K32, transfer constant for the sclera-choroid-RPE from the retina; K30, elimination rate constant from the retina; K34, rate constant for transfer of drug from the retina into the distribution compartment; K43, rate constant for transfer of drug from the distribution compartment into the retina; Krel, rate constant for dissolution/release of celecoxib from the formulation. The observed data are expressed as the mean \pm SD for $n = 4$.

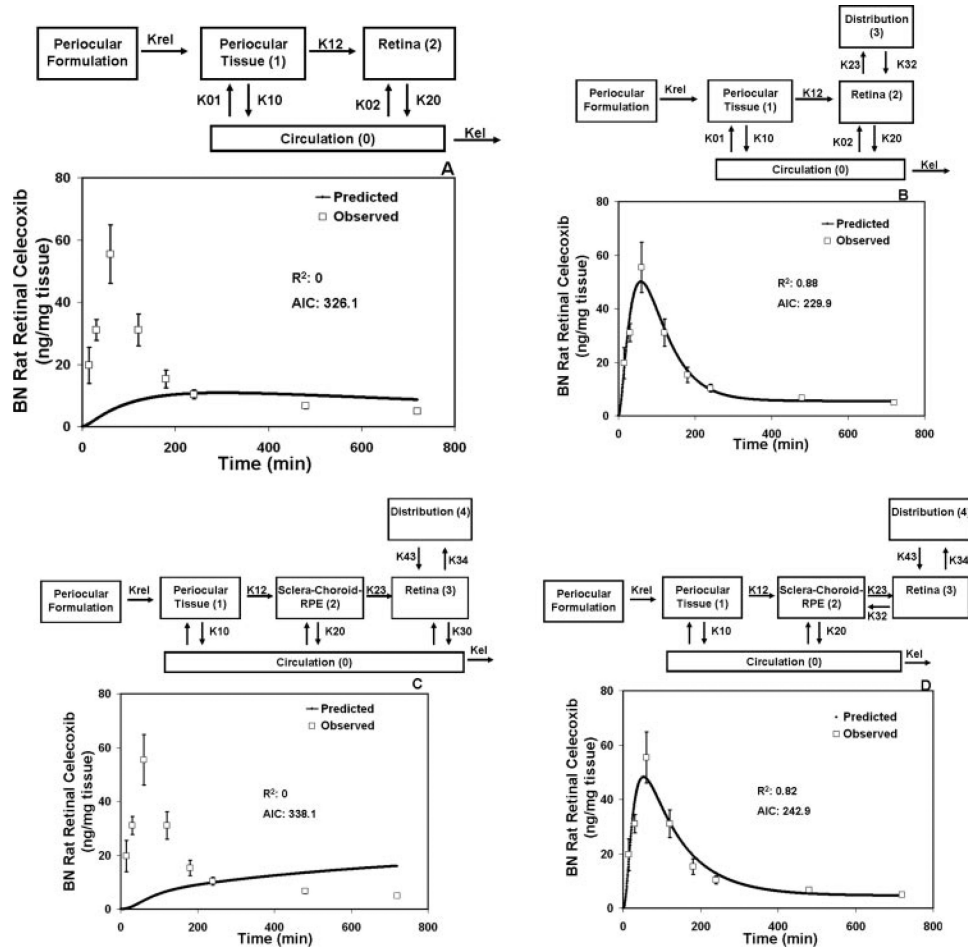


Figure 6. Model-predicted and observed concentrations of celecoxib in the retina after administration of 3 mg celecoxib by periocular injection to BN rats using the recirculation models. **(A)** Four-compartment model with dissolution/release step for the formulation and inclusion of a circulation compartment. **(B)** Five-compartment model with dissolution/release step for the formulation, a distribution compartment for the retina, and inclusion of a circulation compartment. **(C)** Six-compartment model with dissolution/release step for the formulation, a distribution compartment for the retina and inclusion of a circulation compartment and a transfer compartment representing the sclera-choroid-RPE. **(D)** Six-compartment model with dissolution/release step for the formulation, a distribution compartment for the retina and inclusion of a circulation compartment and a transfer compartment representing the sclera-choroid-RPE with no elimination from the retina. **(A, B)** K_{10} , transfer constant for transfer of drug from the periocular site to the circulation; K_{01} , transfer constant for transfer of the drug from the circulation to the periocular site; K_{12} , absorption rate constant for retina; K_{20} , rate constant for transfer of the drug from the retina to the circulation compartment; K_{02} , rate constant for transfer of the drug from the circulation compartment to the retina; K_{23} , rate constant for transfer of the drug from the retina to the distribution compartment; K_{32} , rate constant for transfer of drug from the distribution compartment to the retina; K_{el} , elimination rate constant from the circulation; K_{rel} , rate constant for dissolution/release from the formulation. **(C, D)** K_{10} , transfer constant for transfer of drug from the periocular site to the circulation; K_{01} , transfer constant for transfer of the drug from the circulation to the periocular site; K_{12} , absorption rate constant for sclera-choroid-

RPE; K_{20} , rate constant for transfer of the drug from the sclera-choroid-RPE to the circulation compartment; K_{02} , rate constant for transfer of the drug from the circulation compartment to the sclera-choroid-RPE; K_{23} , rate constant for absorption of drug into the retina from the sclera-choroid-RPE; K_{32} , rate constant for transfer of drug from the retina to the sclera-choroid-RPE; K_{30} , rate constant for transfer of drug from the retina to the circulation compartment; K_{03} , rate constant for the transfer of drug from the circulation compartment to the retina; K_{34} , rate constant for transfer of drug from the retina to the distribution compartment; K_{43} , rate constant for transfer of drug from the distribution compartment to the retina; K_{el} , elimination rate constant from the circulation; K_{rel} , rate constant for dissolution/release from the formulation. The observed data are expressed as the mean \pm SD for $n = 4$.

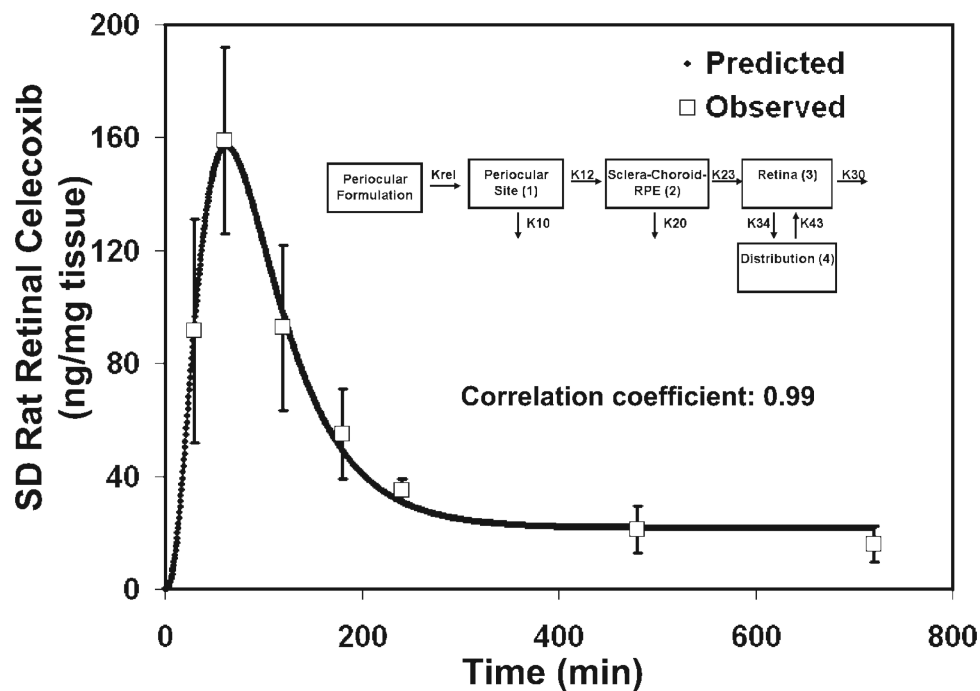


Figure 7. Model-predicted and observed concentrations of celecoxib in the retina after administration of 3 mg celecoxib by periocular injection to SD (nonpigmented) rats. The data were fit to the finalized model selected for retinal kinetics and shown in Figure 5E. Excellent correlation was found between the predicted and observed data. The observed data are expressed as the mean \pm SD for $n = 3$.

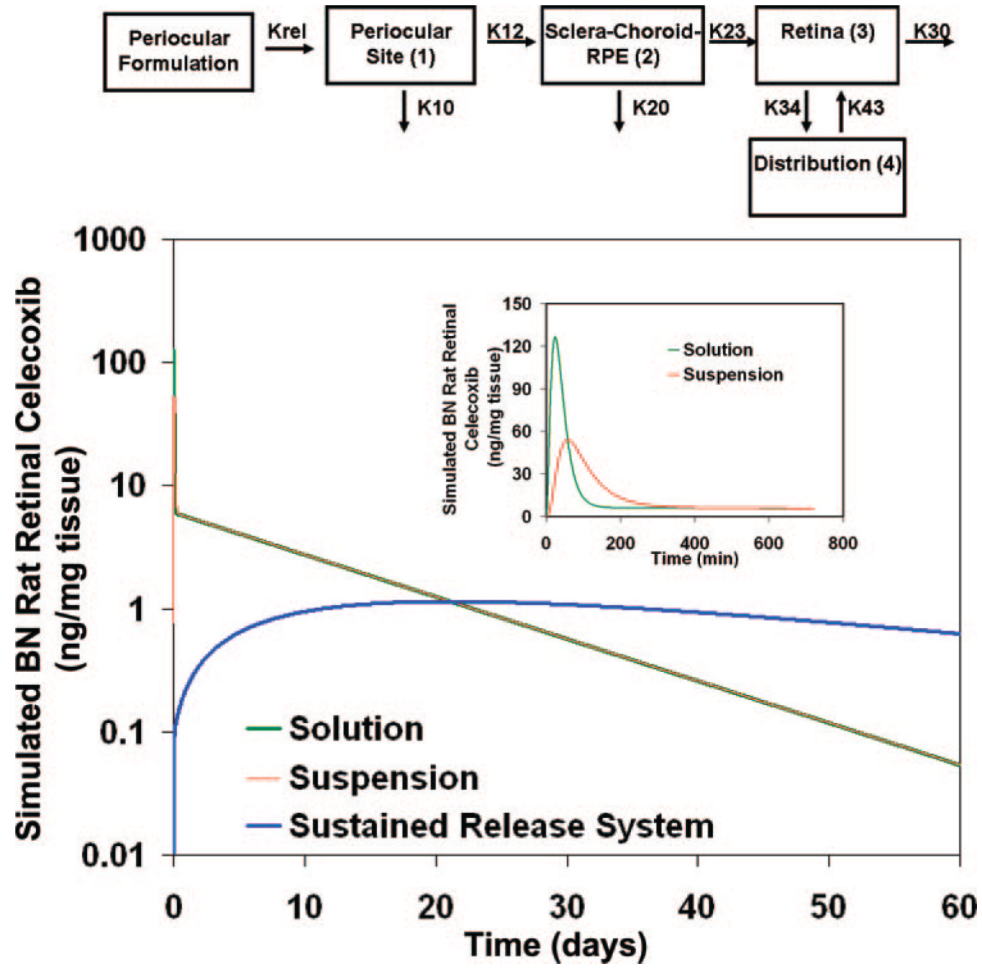


Figure 8. Simulation of celecoxib drug levels in the retina of BN rats by using the parameter estimates in Table 4 and the model in Figure 5E after administration of 3 mg celecoxib by the periocular route as a solution, suspension, or sustained-release system. The sustained-release system was assumed to have a release rate 1000 times less than the release from suspension. *Top:* structural model; *inset:* simulated retinal levels of celecoxib during the initial 12 hours after solution and suspension administration.

Table 1

Parameter Estimates for the Finalized Model for Retinal Pharmacokinetics of Celecoxib after Periocular Administration in Pigmented BN and Nonpigmented SD Rats

Symbol	Meaning	BN Rats	SD Rats
K10	Elimination rate constant from periocular site	0.135	0.134
K12	Absorption rate constant for cornea	1.5e-4	1.3e-4
K20	Elimination rate constant from the cornea	0.177	0.154
Krel	Dissolution/release rate constant from the formulation	0.024	0.025

Data are expressed as minutes⁻¹. The structural model is shown in Figure 1E.

Table 2

Parameter Estimates for Modeling of the Corneal Pharmacokinetics after Subconjunctival Administration of Prednisolone Sodium Succinate in Rabbits

Symbol	Meaning	Value (min^{-1})
K10	Elimination rate constant from the periocular site	0.072
K12	Absorption rate constant for cornea	2.11e-7
K20	Elimination rate constant from the cornea	0.065

The finalized model (Fig. 1E) for corneal pharmacokinetics of celecoxib after periocular administration in rats was used as the model, and curve fitting was performed to obtain the parameter estimates. Since the drug was administered as a solution, the drug dissolution/release step in the model was not included.

Table 3

Parameter Estimates for the Finalized Model for Retinal Pharmacokinetics of Celecoxib after Periocular Administration in Pigmented BN and Nonpigmented SD Rats

Symbol	Meaning	BN rats	SD rats
K10	Elimination rate constant from periocular site	0.123	0.115
K12	Absorption rate constant for sclera-choroid-RPE (transfer compartment)	3.61e-4	6.81 e-4
K20	Elimination rate constant from the sclera-choroid-RPE (transfer compartment)	0.035	0.038
K23	Absorption rate constant for retina from the sclera-choroid-RPE (transfer compartment)	0.061	0.031
K30	Elimination rate constant form the retina	0.002	1.28 e-5
K34	Rate constant for transfer to the distribution compartment from the retina	0.045	0.046
K43	Rate constant for transfer to the retina from the distribution compartment	0.001	0.001
Krel	Rate constant for the release of the drug from the formulation (suspension)	0.017	0.018

The data are expressed as minutes⁻¹. The structural model is shown in Figure 5E.